APL Materials

# Halide vapor phase epitaxial growth of β-$Ga_2O_3$ and α-$Ga_2O_3$ films

Cite as: APL Mater. **7**, 022504 (2019); https://doi.org/10.1063/1.5055680
Submitted: 09 September 2018 • Accepted: 12 November 2018 • Published Online: 11 December 2018

J. H. Leach, K. Udwary, J. Rumsey, et al.

COLLECTIONS

Paper published as part of the special topic on Wide Bandgap Oxides

openaccess

View Online Export Citation CrossMark

ARTICLES YOU MAY BE INTERESTED IN

Perspective: $Ga_2O_3$ for ultra-high power rectifiers and MOSFETS
Journal of Applied Physics **124**, 220901 (2018); https://doi.org/10.1063/1.5062841

MOCVD grown epitaxial $\beta$-$Ga_2O_3$ thin film with an electron mobility of 176 $cm^2$/V s at room temperature
APL Materials **7**, 022506 (2019); https://doi.org/10.1063/1.5058059

Crystal Structure of β-$Ga_2O_3$
The Journal of Chemical Physics **33**, 676 (1960); https://doi.org/10.1063/1.1731237

AMERICAN ELEMENTS
THE ADVANCED MATERIALS MANUFACTURER
The Next Generation of Material Science Catalogs
Now Invent.
www.americanelements.com

AIP Publishing



© 2018 Author(s).

# Halide vapor phase epitaxial growth of β-$Ga_2O_3$ and α-$Ga_2O_3$ films

Cite as: APL Mater. 7, 022504 (2019); doi: 10.1063/1.5055680
Submitted: 9 September 2018 • Accepted: 12 November 2018 •
Published Online: 11 December 2018

J. H. Leach, K. Udwary, J. Rumsey, G. Dodson, H. Splawn, and K. R. Evans

## AFFILIATIONS

Kyma Technologies, Inc., 8829 Midway West Road, Raleigh, North Carolina 27617, USA

## ABSTRACT

Halide vapor phase epitaxy was used to grow homoepitaxial films of β-$Ga_2O_3$ on bulk (010) crystals and heteroepitaxial films of α-$Ga_2O_3$ on c-plane sapphire substrates. The β-$Ga_2O_3$ substrates were prepared prior to growth to remove sub-surface damage and to apply various miscuts to their surfaces. Structural and electrical properties were found to be most impacted by the crystallinity of the β-$Ga_2O_3$ substrate itself, while the surface morphology was found to be most impacted by the miscut of the substrate. The appropriate choice of growth conditions and the miscut appear to be critical to realizing smooth, thick (>20 $\mu$m) homoepitaxial films of β-$Ga_2O_3$. The α-$Ga_2O_3$ films were grown on commercially available c-plane sapphire substrates, and the film morphology was found to be strongly impacted by the surface finish of the sapphire substrates. The α-$Ga_2O_3$ films were found to be smooth and free of additional phases or crystal twinning when the sapphire was sufficiently polished prior to growth.

© 2018 Author(s). *All article content, except where otherwise noted, is licensed under a Creative Commons Attribution (CC BY) license (http://creativecommons.org/licenses/by/4.0/).* https://doi.org/10.1063/1.5055680

Monoclinic β-$Ga_2O_3$ and rhombohedral α-$Ga_2O_3$ have recently emerged as a promising materials for "ultrawide" bandgap electronics for next-generation high voltage lateral and vertical power switching devices, thanks to their large bandgaps (4.9 eV and 5.3 eV, respectively),[1,2] high expected critical breakdown field (8 MV/cm and 10 MV/cm, respectively), and their accordingly large high voltage and high frequency Baliga figures of merit.[3,4] Early research in the thermodynamically stable β-$Ga_2O_3$ was largely pointed toward its use as a transparent conducting oxide material, especially for UV applications,[5] but more recently researchers have demonstrated several $Ga_2O_3$-based devices with promising performances including SBDs,[6] MESFETS,[7] and MOSFETS[8,9] from homoepitaxial β-$Ga_2O_3$ as well as SBDs,[10,11] and MOSFETS[12] from α-$Ga_2O_3$ on sapphire substrates.

Molecular beam epitaxy (MBE)[13] and metal-organic chemical vapor deposition (MOCVD)[14] have been used to homoepitaxially grow thin films of high structural quality β–$Ga_2O_3$. MBE is an excellent technique for research purposes, but the ultra-high vacuum levels required of it, and the relatively low growth rates (<1 $\mu$m/h) associated with MBE call into question its ability to be scaled commercially, not to mention its ability to be utilized for thick (tens of microns) drift regions which will be required of the high voltage vertical devices which are especially well-suited to the $Ga_2O_3$ material system. MOCVD, on the other hand, can likely be pushed to growth rates as high as perhaps 10 $\mu$m/h for β-$Ga_2O_3$, but by the nature of the metalorganic precursors for the group-III elements, material grown by MOCVD will always suffer from the potential for inadvertently high H- and C- concentrations. Until recently, the ability to achieve high quality β-$Ga_2O_3$ films with free carrier concentrations $<1\times10^{17}$ $cm^{-3}$ remained challenging;[15] however, recent results have exhibited high quality films with $N_D - N_A$ values as low as $5\times10^{15}$ $cm^{-3}$ and a corresponding mobility of 174 $cm^2$ $V^{-1}$ $s^{-1}$.[16] Such results are a testament to well-controlled concentrations of unintentional donors (i.e., Si) as well as compensating gallium vacancies[17] or carbon[18] (C being unavoidable in the MOCVD technique).

For thick films that are required for high voltage vertical switching devices, a growth technique which can achieve both high and low growth rates as well as high chemical purity (free of C and H) is desired. Halide vapor phase epitaxy (HVPE) is such a technique and indeed has been validated by


© Author(s) 2018

several groups through the demonstration of high voltage diodes, typically using (001)-oriented β-$Ga_2O_3$ substrates.[6,19,20] To our knowledge, growth by HVPE on (010) β-$Ga_2O_3$ substrates has not been reported, possibly because of the roughnesses associated with growth on this plane when growing on on-axis substrates using this technique. In this work, we outline several issues related to surface preparation which must be addressed in order to realize the promise of the HVPE technique to achieve high quality, high growth rate, and controlled doping for growth of smooth homoepitaxial (010) β-$Ga_2O_3$ films. Additionally, we demonstrate HVPE for growth of high quality heteroepitaxial (0001) α-$Ga_2O_3$ films on sapphire using $Cl_2/H_2$ as the precursor instead of the previously reported HCl precursor for GaCl generation.[21,22]

Homoepitaxial β-$Ga_2O_3$ films and heteroepitaxial α-$Ga_2O_3$ films were grown in a custom-designed Kyma halide vapor phase epitaxy (HVPE) deposition system using GaCl and $O_2$ precursors. The GaCl vapor was generated using HCl or a combination of $Cl_2/H_2$ with liquid gallium, and $O_2$ wa delivered using air (19.5% $O_2$ in $N_2$, Airgas UN1002). Pure $N_2$ was used as the carrier gas, and the temperatures ranged from 950 °C to 1080 °C for β-$Ga_2O_3$ and from 500 °C to 600 °C for α-$Ga_2O_3$. The β-$Ga_2O_3$ films were grown on bulk (010) substrates produced by either Tamura Corporation or Northrup Grumman Synoptics using HCl as the precursor for GaCl generation for the case of Si-doped β-$Ga_2O_3$ films and either HCl or $Cl_2/H_2$ for GaCl generation for the case of undoped films. $SiH_4$ (0.2% in $N_2$) was used as the dopant for Si-doped films. Undoped α-$Ga_2O_3$ films were grown on commercially available *c*-plane sapphire substrates with a nominal miscut of 0.2° using $Cl_2/H_2$ for GaCl generation. The surfaces of the bulk (010) substrates were prepared by Kyma using a series of lapping steps to impart an intentional miscut to the substrate surface using diamond-based slurries, and the substrates were finished using an alkaline-based chemo-mechanical polishing (CMP) process. The sapphire substrates were used as-received.

Film thickness was assessed after growth by weight using a digital scale with 0.1 mg readability. AFM images were collected from the CMP-polished bulk β-$Ga_2O_3$ wafers using a Pacific Nanotechnology Nano-R system. Nomarski differential interference contrast (NDIC) microscopy was used to assess the surface morphology of the epitaxial films, and images were collected using a Nikon Eclipse L200. Both 2θ − ω and ω rocking curves were collected using a Panalytical X'Pert PRO high-resolution x-ray diffractometer in a double crystal configuration with open detector optics. Carrier density and mobility of the films were characterized via Hall effect measurements in a van der Pauw geometry using a home-built measurement system with an electromagnet from GMW Associates at a magnetic field of 0.5 T.

The preparation of the (010) β-$Ga_2O_3$ substrate surface was found to be critical to being able to achieve high quality homoepitaxial layers when growing by HVPE. When polishing substrates which are sliced from a boule, assessment of subsurface damage is considered as a critical first step to determine the epi-readiness of a surface.[23] Although AFM is typically utilized to look for scratching on the substrate surface, a smooth surface under AFM was found to be a necessary yet insufficient condition for high quality epi. Figure 1 shows a 1 × 1 $\mu$m AFM scan of an (010) β-$Ga_2O_3$ surface after CMP polishing. The surface is featureless and it was difficult to discern any features with the AFM utilized in this study. However, upon growth of a thin (0.5 $\mu$m) undoped film of homoepitaxial β-$Ga_2O_3$ at 1000 °C under a GaCl partial pressure of 0.4 Torr and an $O_2$/GaCl ratio of 0.5, there is a clear difference in the morphology of the epilayer realized from a sufficiently

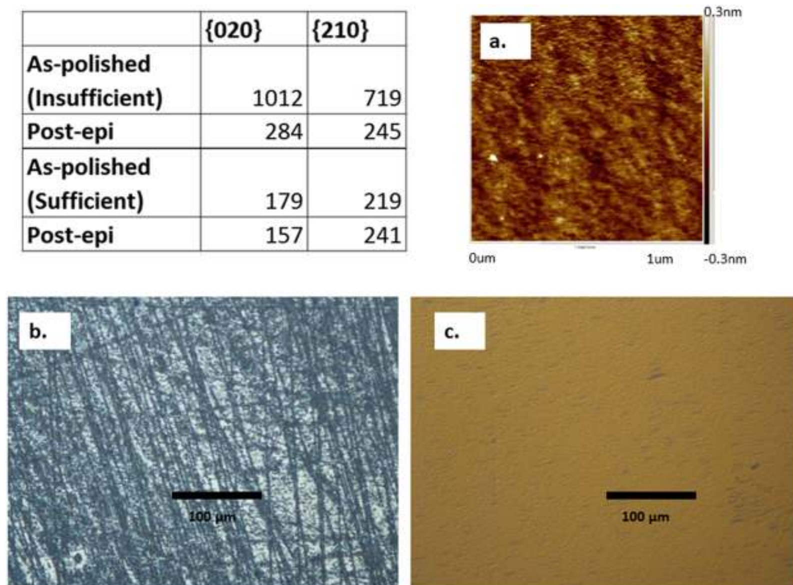

| | {020} | {210} |
|---|---|---|
| As-polished (Insufficient) | 1012 | 719 |
| Post-epi | 284 | 245 |
| As-polished (Sufficient) | 179 | 219 |
| Post-epi | 157 | 241 |



**FIG. 1**. Table of XRD linewidths for as-polished wafers and post-HVPE films using insufficiently polished and sufficiently polished processes. (a) 1 × 1 $\mu$m AFM image of a polished (010) β-$Ga_2O_3$ substrate and optical microscope images after 0.5 $\mu$m of homoepitaxial $Ga_2O_3$ growth using (b) an insufficiently polished and (c) a sufficiently polished substrate.



© Author(s) 2018

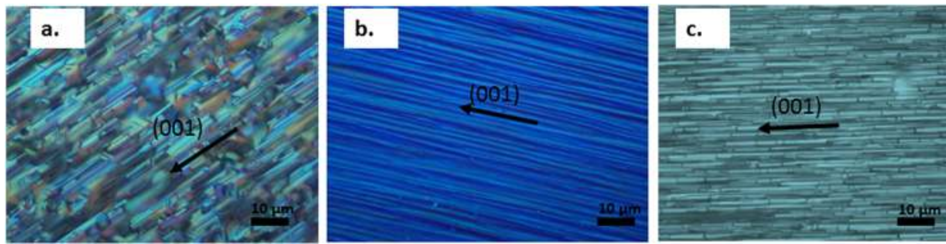


**FIG. 2**. Optical microscope images (at 100×) of films grown under identical growth conditions at 1000 °C on differently prepared bulk (010) substrates. Films were grown for different lengths of time to exaggerate the growth morphology. (a) 2 h of growth resulting in a rough 5.3 $\mu$m thick film on an on-axis (010) substrate. (b) 8 h of growth resulting in 19.6 $\mu$m of growth on a substrate with ∼2° miscut in the (100) direction. (c) 1 h of growth resulting in 1.7 $\mu$m of growth on a substrate with ∼2° miscut in the (001).

polished substrate and an insufficiently polished substrate. The insufficiently polished substrate (which was polished to a finish similar to that shown in the AFM image of Fig. 1) exhibits a large network of scratch-like features after epigrowth, while the epigrowth on the sufficiently polished substrate is free of scratch-like features. We surmise that the insufficiently polished substrate actually had a vast network of sub-surface damage which was not evident by AFM prior to epigrowth. Note that the only difference between these two samples was related to optimizing the relative polishing times of the various polishing steps. In addition to exhibiting vastly different morphologies, the XRD linewidths (defined as the full-width at half-maximum) of the wafers after insufficient or sufficient polishing processes were significantly different (see the table in Fig. 1) and also the {020} reflections measured after growth were significantly broader for the film grown on the insufficiently polished substrate vs the sufficiently polished substrate (see table). Curiously, the XRD linewidths associated with the {210} reflections were much more similar after growth, which is notable considering that the value of 2θ is larger for {020} than that for {210} (and accordingly the sampling depth is larger for the {020} reflection). Regardless, the point here is that a smooth surface morphology after polishing is a necessary but insufficient condition for realizing smooth epigrowth. It should also be noted that the XRD linewidth of the sufficiently polished substrate was nearly the same before and after the epigrowth, indicating that the HVPE growth process provides a good replication of the underlying crystal structure.

In addition to the requirements for surface preparation associated with the removal of sub-surface damage, the morphology of homoepitaxial HVPE growth of (010) β-$Ga_2O_3$ appears to be strongly affected by the surface miscut of the (010) substrate. Since growth rates in the (100) and (001) directions differ, it can be expected that the development of a rough or textured surface morphology would manifest, especially for the growth of relatively thick films under a nearly equilibrium growth process such as HVPE.[24] Accordingly, we prepared a set of nominally (010) β-$Ga_2O_3$ substrates and grew relatively thick undoped films to investigate the surface morphology of the epilayer. Figure 2 shows the microscope images of epilayers grown under identical conditions at 1000 °C using an HCl precursor under a GaCl partial pressure of 0.4 Torr and an $O_2$/GaCl ratio of 0.5 on an on-axis substrate, a substrate which was miscut ∼2° toward (100), and a substrate which was miscut ∼2° toward (001). The growth times were varied to exaggerate the surface morphology. The epilayer on the on-axis substrate exhibits a very rough morphology at a growth thickness of 5.3 $\mu$m. Even at thicknesses <1 $\mu$m, growth using on-axis substrates exhibits significant roughness; however, despite the relatively poor morphology associated with the growth on-axis, 1 $\mu$m thick films grown on on-axis substrates exhibit very high crystalline quality, as evidenced by the narrow XRD linewidths [28 arc sec for the (−820) reflection] and nearly ideal lattice parameters with $a$ = 12.2142 Å ± 0.0013 Å; $b$ = 3.0373 Å ± 0.0001 Å; c = 5.7983 Å ± 0.0018 Å; and $\beta$ = 103.83° ± 0.023°. Growth on substrates which were miscut in the (100) direction exhibited the smoothest morphologies [Fig. 2(b)]. Growth of films up to 19.6 $\mu$m could be realized without severe degradation of the surface morphology as was evident for growth using on-axis or substrates with a miscut in the (001) direction. When miscut in the (001) direction, the growth appears to have a morphology very similar to that associated with growth using an on-axis substrate [Fig. 2(c)]. Figure 2(c) shows that the 1.7 $\mu$m thick

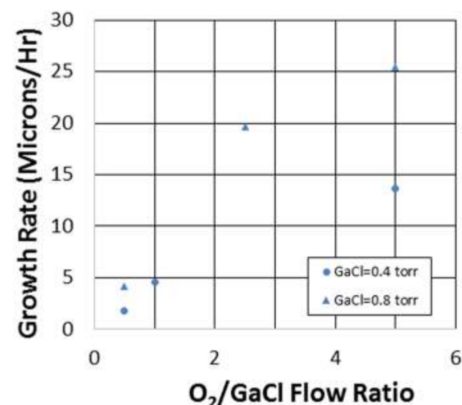


**FIG. 3**. Survey of several of the growth rates achieved for homoepitaxial β-$Ga_2O_3$ films grown by HVPE.


© Author(s) 2018

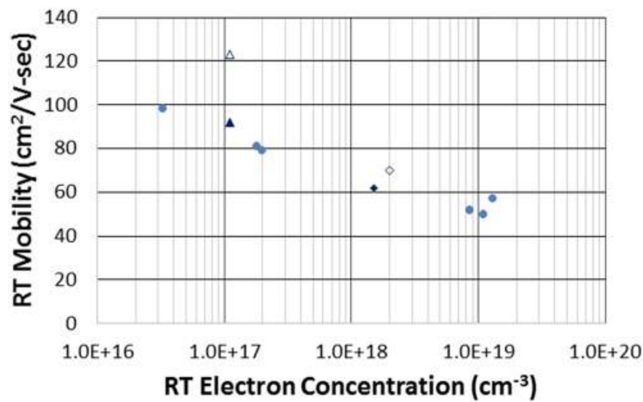


**FIG. 4**. Survey of room temperature mobilities vs. electron concentrations for various films grown on bulk β-$Ga_2O_3$. The triangles and diamonds represent films grown under identical conditions except that the diamonds represent intentionally Si-doped films, while the triangles represent unintentionally doped films. The open triangle and open diamond represent growths on bulk substrates with higher structural quality (exhibiting linewidths < 100 arc sec for {020} reflections).

epilayer grown on a (001)-directed miscut exhibits the same striated surface morphology as that associated with homoepitaxy on on-axis (010) β-$Ga_2O_3$ with the striated features eventually giving rise to a "bamboo" morphology. Upon further growth after the "bamboo" structure appears, additional grains appear at the nodes [the nodes are obvious in Fig. 2(c), and the additional grains are just beginning to form], which gives rise to polycrystalline inclusions in the film [the out-of-focus grains are obvious in Fig. 2(a)].

High growth rates and good electrical quality films are achievable using the HVPE technique for homoepitaxial β-$Ga_2O_3$ growth if the sub-surface damage and surface miscut are appropriately controlled. Figure 3 shows the growth rates realized for two sets of samples grown on bulk substrates using HCl as the precursor under two GaCl partial pressures using various $O_2$/GaCl ratios. Good control of the growth rates was achieved, and the ability to realize growth rates >25 $\mu$m/h bodes well for the growth of thick films for power switching applications. Figure 4 shows several room temperature mobilities along with their associated electron concentrations for films grown on nominally on-axis bulk substrates using different growth conditions. All films exhibiting room temperature electron concentrations $>1 \times 10^{18}$ $cm^{-3}$ were grown using $SiH_4$ as the dopant, and the films exhibiting electron concentrations $<1 \times 10^{18}$ $cm^{-3}$ were grown without intentional doping. The films depicted using triangles or diamonds were grown under identical growth conditions at 1000 °C using HCl as the precursor with an $O_2$/GaCl ratio of 0.5 with diamonds representing films grown using $SiH_4$ and triangles representing films without intentional doping. The triangles and diamonds were grown using different structural quality substrates with open markers representing substrates with {020} linewidths < 100 arc sec and closed markers representing substrates with {020} linewidths > 100 arc sec. Considering that the other growth parameters were the same, the differences in mobility between the two triangles and the two diamonds can be attributed to the differences in the structural quality of the starting substrates; growth on higher structural quality substrates yields higher electrical quality films. The highest mobility realized was 123 $cm^2$ $V^{-1}$ $s^{-1}$ at a carrier concentration of $1.1 \times 10^{17}$ $cm^{-3}$ using a high quality substrate (open triangle). The closed circles all represent films grown on substrates with {020} linewidths > 100 arc sec and under varied growth conditions using $Cl_2/H_2$

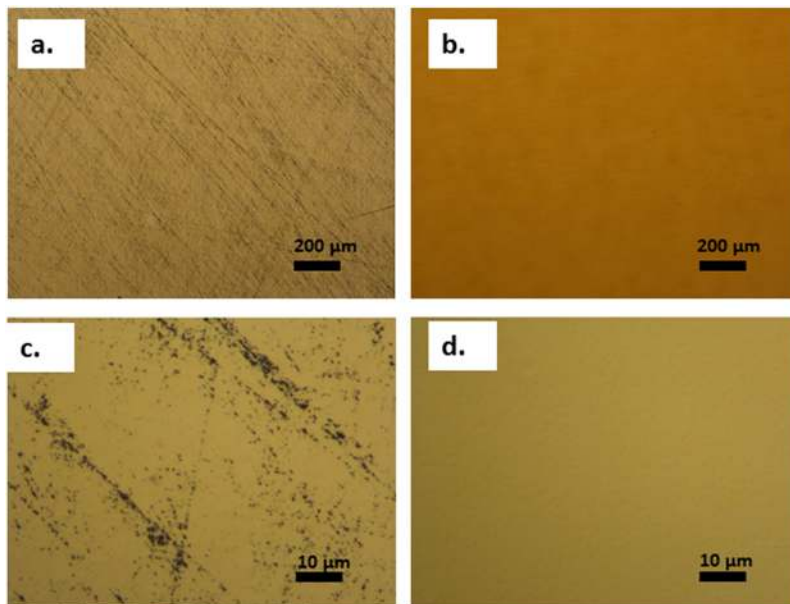


**FIG. 5**. Microscope images at 20× [(a) and (b)] and 100× [(c) and (d)] of 1 $\mu$m thick films of α–$Ga_2O_3$ grown on properly polished [(b) and (d)] and unsuitably polished [(a) and (c)] c-plane sapphire substrates.


© Author(s) 2018

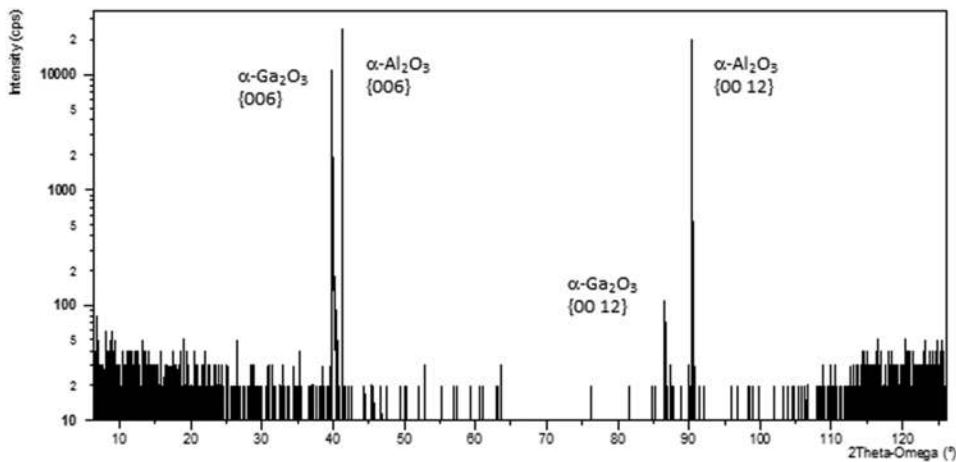


**FIG. 6**. Broad XRD 2θ − ω scan of a 1 $\mu$m thick film of $Ga_2O_3$ on sapphire exhibiting only the α-phase.

as the GaCl precursor and various $O_2$/GaCl ratios (for the films exhibiting electron concentrations $<1 \times 10^{18}$ cm$^{-3}$) or using HCl as the GaCl precursor and using different $SiH_4$ flows (the films exhibiting electron concentrations $>1 \times 10^{18}$ cm$^{-3}$). Further studies highlighting differences in the film properties when using $Cl_2/H_2$ as compared to HCl for the GaCl generation are forthcoming and will be reported elsewhere.

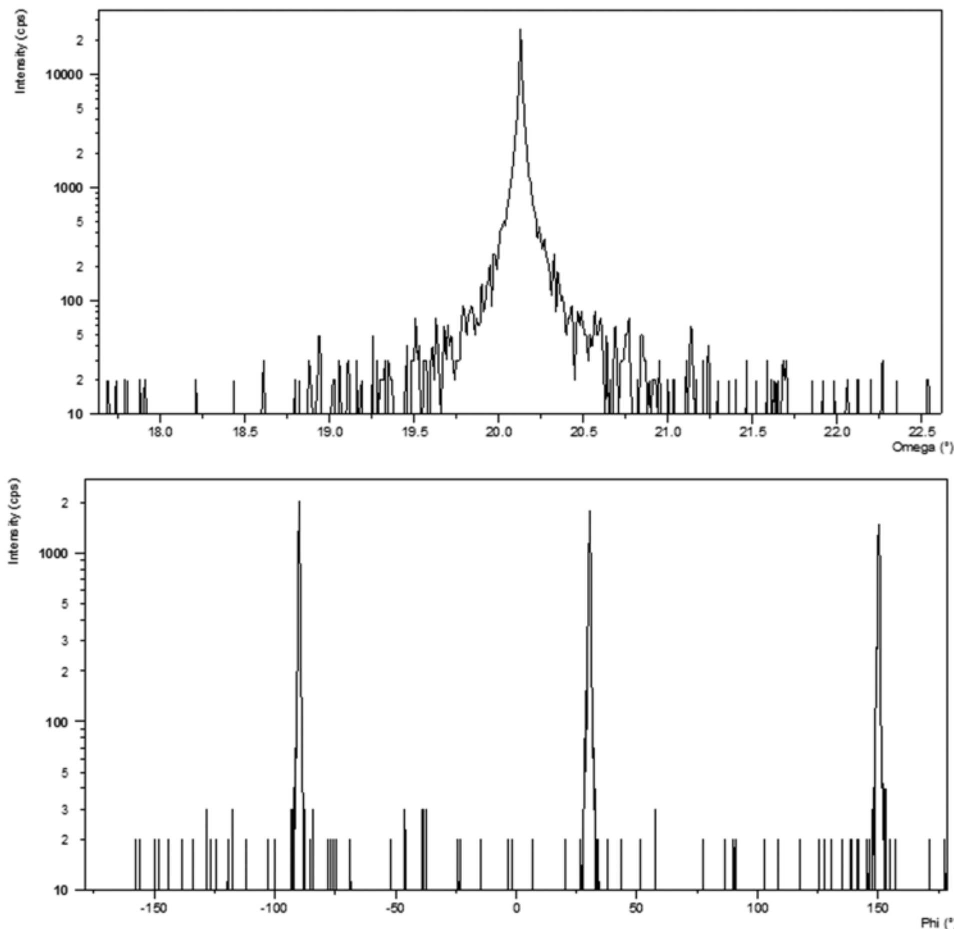


**FIG. 7**. (Top) XRD rocking curve about the {006} reflection of the 1 $\mu$m thick film of α–$Ga_2O_3$ on sapphire showing a linewidth of 79 arc sec. (Bottom) XRD $\phi$-scan about the {204} reflection of a 1 $\mu$m thick film of α–$Ga_2O_3$ on sapphire showing a three-fold symmetry and no evidence of twinning in the film.


© Author(s) 2018

The metastable α-$Ga_2O_3$ has a higher crystallographic point group symmetry as well as a wider bandgap than β-$Ga_2O_3$ and thus is more interesting for device applications than β-$Ga_2O_3$; however, since it cannot be grown from the melt like β-$Ga_2O_3$, it requires a foreign substrate upon which to grow. Commonly used c-plane sapphire substrates have the same point group symmetry as α-$Ga_2O_3$ and accordingly are suitable candidates for the development of α-$Ga_2O_3$ epilayers. As was the case with β-$Ga_2O_3$, the surface preparation of the sapphire substrate is important. Although sapphire has become inexpensive and ubiquitous throughout the market, one can still be challenged to polish it appropriately. Figure 5 shows microscope images from a pair of identical 1 $\mu$m thick undoped HVPE films of α-$Ga_2O_3$ grown on sapphire substrates procured from two different sapphire vendors. The growths were performed in 10 min (e.g., a growth rate of 6 $\mu$m/h) using the same reactor as that utilized for β-$Ga_2O_3$ growth at 550 °C and using $Cl_2/H_2$ for the generation of GaCl instead of HCl and using an $O_2$/GaCl ratio of 0.5. The images on the left clearly show scratch-like features in the epi, while the images on the right are smooth and free of scratch-like features. It is possible that AFM or some other techniques could be used to screen the sapphire substrates prior to growth to ensure that one is growing on a suitably prepared substrate.

Nevertheless, using an appropriately polished sapphire substrate or a qualified vendor of featureless sapphire substrates, α-$Ga_2O_3$ films can be made to grow in a single phase with high quality and without crystal twinning in the film. This is evidenced from the set of reflections observed in the broad 2θ – ω scan given in Fig. 6 which only exhibits peaks associated with the c-plane sapphire (both (006) and (00 12) as shown in the figure) as well as α-phase $Ga_2O_3$ [each correlated to the underlying α-phase $Al_2O_3$, (006) and (00 12)]. Figure 7 shows that α-$Ga_2O_3$ has an XRD linewidth for the (006) reflection of 79 arc sec and a linewidth for the (204) reflection of 1690 arc sec. In this skew-symmetric geometric condition, only three peaks can be observed when rotating in phi about (204), which indicates high crystalline quality and no twinning. The (006) linewidth is significantly narrower than previous reports of α-$Ga_2O_3$ using HVPE.[21] The reason for this is unclear but may be related to the use of $Cl_2/H_2$ in lieu of HCl or simply due to the relatively slow growth rate of α-$Ga_2O_3$ as compared to the previous report. A doping study and corresponding analysis would be the appropriate next step to better understand the electrical properties of these films, but, nevertheless, their crystalline quality is encouraging for additional attention.

Halide vapor phase epitaxy (HVPE) was used to prepare high quality films of both β-$Ga_2O_3$ and α-$Ga_2O_3$ homoepitaxially and heteroepitaxially, respectively. The surface preparation in terms of sub-surface damage for both phases as well as the substrate miscut and its direction for the β-$Ga_2O_3$ phase was shown to be critical to realizing high quality films with a suitable surface morphology to realize thick films for the future development of power devices.

This research was partially supported by the Office of Naval Research under Contract No. N00014-16-P-2031 and the Air Force Office of Scientific Research under Contract No. FA9550-17-P-0012. The authors would also like to thank N. Mahadik and M. Tadjer at the Naval Research Labs for the lattice parameter measurements and S. Mou and A. Neal at the Air Force Research Labs for several of the Hall measurements.

## REFERENCES

[1] H. H. Tippins, "Optical absorption and photoconductivity in the band edge of β-$Ga_2O_3$," Phys. Rev. **140**, A316 (1965).

[2] D. Shinohara and S. Fujita, "Heteroepitaxy of corundum-structured α-$Ga_2O_3$ thin films on α-$Al_2O_3$ substrates by ultrasonic mist chemical vapor deposition," Jpn. J. Appl. Phys., Part 1 **47**, 7311 (2008).

[3] J. Y. Tsao, S. Chowdhury, M. A. Hollis, D. Jena, N. M. Johnson, K. A. Jones, R. J. Kaplar, S. Rajan, C. G. Van de Walle, E. Bellotti, C. L. Chua, R. Collazo, M. E. Coltrin, J. A. Cooper, K. R. Evans, S. Graham, T. A. Grotjohn, E. R. Heller, M. Higashiwaki, M. S. Islam, P. W. Juodawlkis, M. A. Khan, A. D. Koehler, J. H. Leach, U. K. Mishra, R. J. Nemanich, R. C. N. Pilawa-Podgurski, J. B. Shealy, Z. Sitar, M. J. Tadjer, A. F. Witulski, M. Wraback, and J. A. Simmons, "Ultrawide-bandgap semiconductors: Research opportunities and challenges," Adv. Electron. Mater. **4**, 1600501 (2018).

[4] M. Higashiwaki, K. Sasaki, H. Murakami, Y. Kumagai, A. Koukitu, A. Kuramata, T. Masui, and S. Yamakoshi, "Recent progress in $Ga_2O_3$ power devices," Semicond. Sci. Technol. **31**, 034001 (2016).

[5] H. Hosono, in *Handbook of Transparent Conductors*, edited by D. S. Ginley (Springer, New York, 2010).

[6] H. Murakami, K. Nomura, K. Goto, K. Sasaki, K. Kawara, Q. T. Thieu, R. Togashi, Y. Kumagai, M. Higashiwaki, A. Kuramata, S. Yamakoshi, B. Monemar, and A. Koukitu, "Homoepitaxial growth of β-$Ga_2O_3$ layers by halide vapor phase epitaxy," Appl. Phys. Express **8**, 015503 (2015).

[7] M. Higashiwaki, K. Sasaki, T. Kamimura, T. Masui, and S. Yamakoshi, "Gallium oxide ($Ga_2O_3$) metal-semiconductor field-effect transistors on single-crystal β-$Ga_2O_3$ (010) substrates," Appl. Phys. Lett. **100**, 013504 (2012).

[8] A. J. Green, K. D. Chabak, E. R. Heller, R. C. Fitch, Jr., M. Baldini, A. Fiedler, K. Irmscher, G. Wagner, Z. Galazka, S. E. Tetlak, A. Crespo, K. Leedy, and G. H. Jessen, "3.8 MV/cm breakdown strength of MOVPE-grown Sn-doped β-$Ga_2O_3$ MOSFETs," IEEE Electron Device Lett. **37**, 902 (2016).

[9] M. H. Wong, Y. Nakata, A. Kuramata, S. Yamakoshi, and M. Higashiwaki, "Enhancement-mode $Ga_2O_3$ MOSFETs with Si-implanted source and drain," Appl. Phys. Express **10**, 041101 (2017).

[10] K. Kaneko, S. Fujita, and T. Hitora, "A power device material of corundum-structured a-$Ga_2O_3$ fabricated by MIST EPITAXY® technique," Jpn. J. Appl. Phys., Part 2 **57**, 02CB18 (2018).

[11] M. Oda, R. Tokuda, H. Kambara, T. Tanikawa, T. Sasaki, and T. Hitora, "Schottky barrier diodes of corrundum-structured gallium oxide showing on-resistance of 0.1 mΩ $cm^2$ grown by MIST EPITAXY®," Appl. Phys. Express **9**, 021101 (2016).

[12] See http://rocakk.sakura.ne.jp/index/struct/wp-content/uploads/79cd9d2dfa54a771f642e008cc4f9cb0.pdf for FLOSFIA press release, 13 July 2018; Accessed 29 August 2018.

[13] M. Y. Tsai, O. Bierwagen, M. E. White, and J. S. Speck, "Beta-$Ga_2O_3$ growth by plasma-assisted molecular beam epitaxy," J. Vac. Sci. Technol., A **28**, 354 (2010).

[14] G. Wagner, M. Baldini, D. Gogova, M. Schmidbauer, R. Schweski, M. Albrecht, Z. Galazka, D. Klimm, and R. Fornari, "Homoepitaxial growth of beta-$Ga_2O_3$ layers by metal-organic vapor phase epitaxy," Phys. Status Solidi A **211**, 27 (2014).

[15] M. Baldini, M. Albrecht, A. Fiedler, K. Irmscher, R. Schewski, and G. Wagner, "Si- and Sn-doped homoepitaxial β-$Ga_2O_3$ layers grown by MOVPE on (010)-oriented substrates," ECS J. Solid State Sci. Technol. **6**, Q3040 (2017).


© Author(s) 2018

[16]A. Osinski, "Device quality β-$(Al_xGa_{1-x})_2O_3$/β-$Ga_2O_3$ heterostructures grown by MOCVD," in GOX 2018, Columbus, OH, USA, 16 August 2018.
[17]E. Korhonen, F. Toumisto, D. Gogova, G. Wagner, M. Baldini, Z. Galazka, R. Schweski, and M. Albrecht, "Electrical compensation by Ga vacancies in $Ga_2O_3$ films," Appl. Phys. Lett. **106**, 242103 (2015).
[18]D. Gogova, M. Schmidbauer, and A. Kwasniewski, "Homo- and heteroepitaxial growth of Sn-doped beta-$Ga_2O_3$ layers of MOVPE," CrystEngComm **17**, 6744 (2015).
[19]K. Konishi, K. Goto, H. Murakami, Y. Kumagai, A. Kuramata, S. Yamakoshi, and M. Higashiwaki, "1-kV vertical $Ga_2O_3$ field-plated Schottky barrier diodes," Appl. Phys. Lett. **110**, 103506 (2017).
[20]J. Yang, F. Ren, M. Tadjer, S. J. Pearton, and A. Kuramata, "$Ga_2O_3$ Schottky rectifiers with 1 ampere forward current, 650 V reverse breakdown and 26.5 MW $cm^{-2}$ figure-of-merit," AIP Adv. **8**, 055026 (2018).
[21]Y. Oshima, E. G. Víllora, and K. Shimamura, "Halide vapor phase epitaxy of twin-free a-$Ga_2O_3$ on sapphire (0001) substrates," Appl. Phys. Express **8**, 055501 (2015).
[22]Y. Yao, S. Okur, L. A. M. Lyle, G. S. Tompa, T. Salagaj, N. Sbrockey, R. F. Davis, and L. M. Porter, "Growth and characterization of α-, β-, and ε-phases of $Ga_2O_3$ using MOCVD and HVPE techniques," Mater. Res. Lett. **6**, 268 (2018).
[23]J. H. Leach, K. Udwary, T. Schneider, J. D. Blevins, K. R. Evans, G. Foundos, and K. T. Stevens, "Development of homoepitaxial growth of $Ga_2O_3$ by hydride vapor phase epitaxy," in 2017 CS MANTECH Conference, Indian Wells, CA, USA, 25 May 2017.
[24]Y. Oshima, E. G. Villora, and K. Shimamura, "Quasi-heteroepitaxial growth of β-$Ga_2O_3$ on off-angled sapphire (0001) substrates by halide vapor phase epitaxy," J. Cryst. Growth **410**, 53 (2015).


© Author(s) 2018